

## Nonergodicity of Blinking Nanocrystals and Other Lévy-Walk Processes

G. Margolin<sup>1</sup> and E. Barkai<sup>1,2</sup>

<sup>1</sup>*Department of Chemistry and Biochemistry, Notre Dame University, Notre Dame, Indiana 46556, USA*

<sup>2</sup>*Department of Physics, Bar Ilan University, Ramat Gan, Israel 52900*

(Received 17 June 2004; published 2 March 2005)

We investigate the nonergodic properties of blinking nanocrystals modeled by a Lévy-walk stochastic process. Using a nonergodic mean field approach we calculate the distribution functions of the time averaged intensity correlation function. We show that these distributions are not delta peaked on the ensemble average correlation function values; instead they are W or U shaped. Beyond blinking nanocrystals our results describe ergodicity breaking in systems modeled by Lévy walks, for example, certain types of chaotic maps and spin dynamics to name a few.

DOI: 10.1103/PhysRevLett.94.080601

PACS numbers: 05.40.Fb, 02.50.-r, 78.67.Bf

Time series of many systems exhibit intermittency, where at random times the system will switch from state *on* (or up) to state *off* (or down) and vice versa. Examples include currents in ion channels [1], flows in chaotic maps [2], and dynamics of spin models [3], e.g., in spin glasses [4]. These diverse systems may display Lévy statistics [5], where sojourn times of one of the states or both are described by power law distributions. Recently, intermittency was found also for blinking nanocrystals (NCs) [6–10] where the system jumps between an on fluorescent state and an off state. One method to characterize such time series uses time average (TA) correlation functions, e.g., of the fluorescence intensity for the blinking NCs. Interestingly, the experiments of [6,7] show that the time average correlation functions exhibit a nonergodic behavior (see details below). What are the nonergodic properties of the correlation functions and how should they be characterized are open questions that we address in this Letter. To be specific, we will consider the phenomenology of blinking nanocrystals; however, with minor modifications our work can apply to other systems.

Consider a fluorescent intensity trajectory  $I(t)$ , recorded in a time interval  $(0, T')$ . A standard method of analyzing blinking intensity signals is to define a threshold  $I_{\text{th}}$  and define two states: on if  $I(t) > I_{\text{th}}$  and off otherwise. For capped NCs [e.g., CdSe(ZnS) core-shell NC], on and off times exhibit power law statistics [9,10], their probability density function (PDF) behaves like  $\psi(\tau) \propto \tau^{-(1+\theta)}$  for large  $\tau$ , and  $\theta < 1$ . For example, in [7] 215 NCs were measured and the exponents  $\theta_{\text{on}} = 0.58 \pm 0.17$  and  $\theta_{\text{off}} = 0.48 \pm 0.15$  were found (note that within error of measurement  $\theta_{\text{on}} = \theta_{\text{off}} = \theta \sim 1/2$ ); further, all NCs are reported to be statistically identical. Since  $\theta < 1$  the average on and off times are infinite. The divergence of occupation times naturally leads to nonergodicity in the blinking NCs [6,7] (see also [11] for a related discussion) and also to interesting aging effects [7,12,13]. Other measurements classify the intermittency based on the time average correlation function or the closely related power spectrum [6,14,15].

From a single realization  $I(t)$  we may construct the time averaged correlation function [16,17]

$$C_{\text{TA}}(t', T') = \frac{\int_0^{T'} I(t+t')I(t)dt}{T}, \quad (1)$$

where we denoted  $T = T' - t'$ . We use a simple two state stochastic model which exhibits nontrivial behaviors. The intensity  $I(t)$  jumps between two states  $I(t) = 1$  and  $I(t) = 0$ . At the start of the measurement  $t = 0$  the NC begins in state on  $I(0) = 1$ . The process is characterized based on the sequence  $\{\tau_1^{\text{on}}, \tau_2^{\text{off}}, \tau_3^{\text{on}}, \tau_4^{\text{off}}, \dots\}$  of on and off sojourn times or equivalently according to the dots on the time axis  $t_1, t_2, \dots$ , on which transitions from on to off or vice versa occur. The times  $\tau_i$  are mutually independent and are drawn at random from the PDF  $\psi(\tau)$ . We use  $\psi(\tau) \propto \tau^{-(1+\theta)}$  for large  $\tau$ , where  $0 < \theta < 1$ . Such power law distributions may be viewed as generated by fractional Poisson process [18]. Note that our model describes a Lévy walk, which is an important stochastic model for anomalous diffusion [5,12,19]. Simple physical models for  $\psi(\tau)$  are discussed in [10,12,14]; the exponent  $\theta = 1/2$  can be explained based on a first passage time model of a three dimensional diffusion of charge carriers [12].

In Fig. 1, ten typical simulated correlation functions are plotted, the most striking feature of the figure is that the correlation functions are random (note that the “noise” in these simulations is in fact the true behavior and is not due to numerical problems). These correlation functions are similar to those obtained in the experiment [6]. Mathematically, the question of nonergodicity may be formulated in the following way. Since the process  $I(t)$  is random the time average correlation function  $C_{\text{TA}}(t', T')$  is random. For ergodic processes, and in the long measurement time limit, the distribution of  $C_{\text{TA}}(t', T')$  is delta peaked and centered around the ensemble average correlation function. For nonergodic processes the goal is to obtain the nontrivial limiting distributions of  $C_{\text{TA}}(t', T')$  which differ from the narrowly peaked delta functions found for ergodic processes. In what follows we will

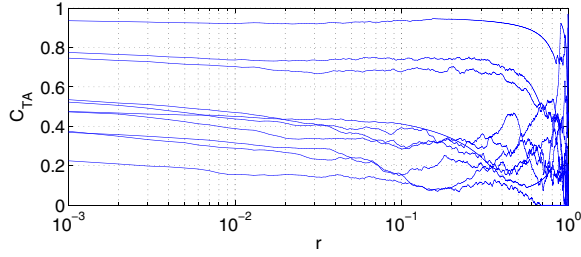


FIG. 1 (color online). Ten numerically generated realizations of the correlation function  $C_{TA}(t', T')$  versus  $r = t'/T'$  for  $\theta = 0.8$  and fixed  $T'$ . The correlation functions exhibit nonergodic behavior and are random. For ergodic processes all ten time averaged correlation functions would follow the same master curve, namely, the ensemble average correlation function.

denote  $P_{C_{TA}(t', T')}(z)$  to be the PDF of  $C_{TA}(t', T')$ ,  $z$  being its possible values;  $0 \leq z \leq 1$  due to Eq. (1).

To start our analysis we rewrite the time average correlation function as

$$C_{TA}(t', T') = \frac{\sum_{i \text{ odd}}^n \int_{t_{i-1}}^{t_i} I(t+t') dt}{T}, \quad (2)$$

where we used the initial condition that  $I(t) = 1$  at time  $t = 0$ . Hence,  $I(t) = 1$  in  $t_{i-1} < t < t_i$  when  $i$  is odd, otherwise it is zero. The summation in Eq. (2) is over odd  $i$ 's, and  $t_n = T$ , namely,  $n - 1$  in Eq. (2) is the random number of transitions in the interval  $[0, T]$ . From Eq. (2) we see that the time averaged correlation function is a sum of the random variables

$$\int_{t_{i-1}}^{t_i} I(t)I(t+t') dt = \begin{cases} \tau_i - t' + I_i t' & i \text{ odd } t_i - t_{i-1} > t' \\ I_i \tau_i & i \text{ odd } t_i - t_{i-1} < t' \\ 0 & i \text{ even,} \end{cases} \quad (3)$$

where

$$I_i = \begin{cases} \frac{\int_{t_i}^{t_i+t'} I(t) dt}{t'} & \text{if } t_i - t_{i-1} > t' \\ \frac{\int_{t_{i-1}+t'}^{t_i} I(t) dt}{\tau_i} & \text{if } t_i - t_{i-1} < t'. \end{cases} \quad (4)$$

The  $I_i$ 's are time averages of the signal  $I(t)$  over periods of length  $t'$  or  $\tau_i = t_i - t_{i-1}$ . Using Eqs. (2) and (3), we find an exact expression for the correlation functions in terms of  $\{\tau_i\}$  and  $\{I_i\}$ ,

$$TC_{TA}(t', T') = \sum_{i \text{ odd}}^n \tau_i - \sum_{\substack{i \text{ odd} \\ \tau_i < t'}}^n (1 - I_i) \tau_i - t' \sum_{\substack{i \text{ odd} \\ \tau_i > t'}}^n (1 - I_i). \quad (5)$$

The first term on the right-hand side of this equation is  $T^+$ , the total time spent in state on in the time interval  $[0, T]$ . In the remaining two terms we have considered sojourn times  $\tau_i$  larger or smaller than  $t'$  separately.

We now illustrate the rich behaviors of the PDF  $P_{C_{TA}(t', T')}(z)$  using numerical simulations, and later we consider the problem analytically. We generate random realization of the process using  $\psi(\tau) = \theta \tau^{-1-\theta}$  for  $\tau > 1$  and show two cases:  $\theta = 0.3$  in Fig. 2 and  $\theta = 0.8$  in Fig. 3. In both figures we vary  $r \equiv t'/T'$ . The diamonds are numerical results which agree very well with the theoretical curves, without any fitting. First consider the case  $r = 0$  in Figs. 2 and 3. For  $\theta = 0.3$  and  $r = 0$  we see from Fig. 2 that the PDF  $P_{C_{TA}(t', T')}(z)$  has a U shape. This is a strong nonergodic behavior, since the PDF does not peak on the ensemble averaged value of the correlation function which is  $1/2$  for this case. On the other hand, when  $\theta = 0.8$  the PDF  $P_{C_{TA}(t', T')}(z)$  has a W shape, a weak nonergodic behavior. To understand the origin of this type of transition note that as  $\theta \rightarrow 0$  we expect the process to be in an on state or an off state for the whole duration of the measurement, hence in that case the PDF of the correlation function will peak on  $C_{TA}(t', T') = 1$  and  $C_{TA}(t', T') = 0$  (i.e., U shape behavior). On the other hand, when  $\theta \rightarrow 1$  we expect a more ergodic behavior, since for  $\theta > 1$  the mean on and off periods are finite, this manifests itself in a peak of the distribution function of  $C_{TA}(t', T')$  on the ensemble average value of  $1/2$  and a W shape PDF emerges. Note that for  $\theta < 1$  there is still statistical weight for trajectories which are on or off for periods which are of the order of the measurement time  $T'$ , hence the distribution of  $C_{TA}(0, T')$  attains its maximum on  $C_{TA}(0, T') = 1$  and  $C_{TA}(0, T') = 0$ . For  $r > 0$  we observe in both figures a nonsymmetrical

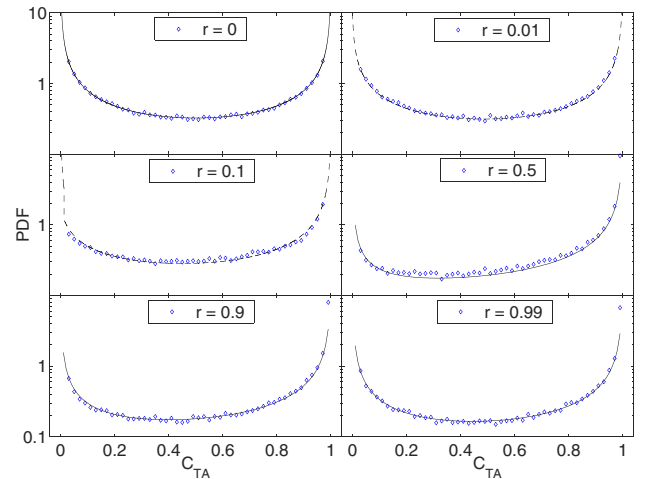


FIG. 2 (color online). The PDF of  $C_{TA}(t', T')$  for  $\theta = 0.3$  and different values of  $r = t'/T'$ . The diamonds are numerical simulations and the curves are analytical expression obtained for  $r = 0$ , Eq. (8) (solid curve),  $r = 0.01, 0.1$ , Eq. (10) (dashed curve), and  $r = 0.5, 0.9, 0.99$ , Eq. (13) (solid curve). In the ergodic phase the PDF of  $C_{TA}(t', T')$  would be peaked around the ensemble average correlation function, which for  $r = 0$  falls on  $1/2$  and for  $t' \rightarrow \infty$  is on  $1/4$  (for any  $r \neq 0$ ). We see that any measurement is highly unlikely to yield the ensemble average when  $\theta = 0.3$ .

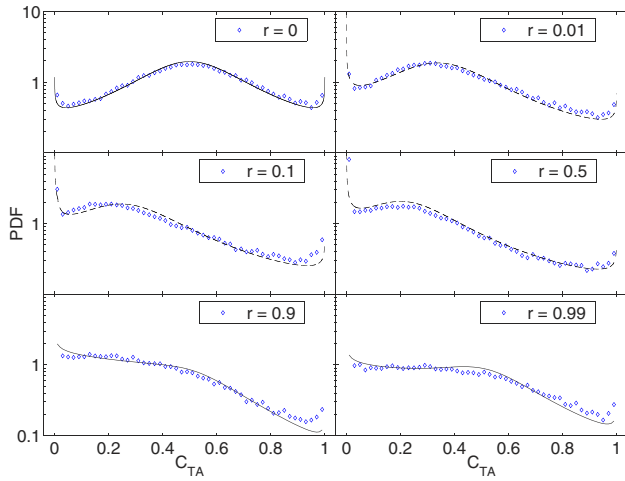


FIG. 3 (color online). Same as Fig. 2. However, now  $\theta = 0.8$  and Eq. (10) is used for  $r = 0.5$ . If compared with the case  $\theta = 0.3$ , the distribution function exhibits a weaker nonergodic behavior; namely, for  $r = 0$  the distribution function peaks on the ensemble average value of  $1/2$ .

shape of the PDF of the correlation function, which will be explained later. We stress that the distributions observed on Figs. 2 and 3 are not a scaling artifact: analogous calculations in the case of  $\theta > 1$  lead in the limit  $T' \rightarrow \infty$  to Dirac  $\delta$  functions instead.

We first consider the nonergodic properties of the correlation function for the case  $t' = 0$ . It is useful to define

$$I_{[a,b]} = \int_a^b I(t) dt / (b - a), \quad (6)$$

the time average intensity between time  $a$  and time  $b > a$ . Using Eq. (5) and for  $t' = 0$  the time averaged correlation function is identical to the time average intensity

$$C_{TA}(0, T) = I_{[0,T]} = \frac{T^+}{T}. \quad (7)$$

The random correlation function  $C_{TA}(0, T)$  has a known asymptotic behavior in the limit  $T \rightarrow \infty$ , found originally by Lamperti [20] (see also [3]). This PDF is denoted with

$$C_{TA}(t', T') \simeq \begin{cases} I_{[0,T]} \{ 1 - (1 - I_{[0,T]}) [(\frac{r}{(1-r)I_{[0,T]}})^{1-\theta} (\frac{\sin \pi \theta}{\pi \theta} + 1) - \frac{\sin \pi \theta}{\pi \theta} \frac{r}{(1-r)I_{[0,T]}}] \} & t' < T^+ \\ I_{[0,T]}^2 & t' > T^+. \end{cases} \quad (10)$$

Equation (10) yields the correlation function. However, unlike standard ergodic theories, the correlation function here is a random function since it depends on  $I_{[0,T]}$ . The distribution of  $C_{TA}(t', T')$  is now easy to find using the chain rule and Eqs. (7), (8), and (10). In Figs. 2 and 3, we plot the PDF of  $C_{TA}(t', T')$  (dashed curves) together with numerical simulations (diamonds) and find excellent agreement between theory and simulation, for the cases where our approximations are expected to hold  $r < 1/2$ . We observe that, unlike the  $r = 0$  case, the PDF of the correlation function exhibits a nonsymmetrical shape. To

$\lim_{T \rightarrow \infty} P_{C_{TA}(0,T)}(z) = l_\theta(z)$ , and

$$l_\theta(z) = \frac{\sin \pi \theta}{\pi} \frac{z^{\theta-1} (1-z)^{\theta-1}}{z^{2\theta} + (1-z)^{2\theta} + 2z^\theta (1-z)^\theta \cos \pi \theta}, \quad (8)$$

for  $0 \leq z \leq 1$ . This function is normalized to 1 for any  $0 < \theta \leq 1$ . The transition between the U shape behavior and the W shape behavior happens at  $\theta_c = 0.5946\dots$ . The Lamperti PDF is shown in Figs. 2 and 3 for the case  $r = 0$ , together with the numerical results.

We now consider an analytical approach for the case  $t' \ll T$ . The behavior of  $P_{C_{TA}(t',T)}(z)$  for  $t' \neq 0$  is nontrivial because the  $I_i$ 's in Eq. (5) depend statistically on the random variables  $\tau_i$ . To treat the problem we use a non-ergodic mean field approximation. We noticed already that  $I_i$  defined in Eq. (4) are short time averages of the intensity; hence, using mean field theory approach we replace the  $I_i$  in Eq. (5) with the *time* average intensity  $I_{[0,T]}$ , *specific for a given realization*. Replacing  $I_i$  with the *ensemble* average intensity is not appropriate. Hence within mean field

$$TC_{TA}(t', T') = I_{[0,T]} T - (1 - I_{[0,T]})(t' N^+ + \Sigma^+), \quad (9)$$

where  $N^+$  is the number of odd (i.e., on) intervals satisfying  $\tau_i \geq t'$  and  $i \leq n$ , while  $\Sigma^+ \equiv \sum_{i \text{ odd}, \tau_i < t'} \tau_i$  is the sum of all odd  $\tau_i < t'$  and  $i \leq n$ .

We now investigate the distribution of  $C_{TA}(t', T')$  using the approximation Eq. (9), leaving certain details of our derivation to a longer publication. First we replace  $N^+$  with its scaling form. Let  $P(\tau > t') = \int_{t'}^\infty \psi(\tau) d\tau$  be the probability of  $\tau$  being larger than  $t'$ , we have  $N^+ \simeq KP(\tau > t')T^+ / \int_0^{T^+} \tau \psi(\tau) d\tau$ , where  $K$  is a constant of order 1, and  $T^+ / \int_0^{T^+} \tau \psi(\tau) d\tau$  is the total number of jumps in time interval  $T^+$ . A more refined treatment yields  $N^+ \simeq \frac{\sin \pi \theta}{\pi \theta} \times [(\frac{T^+}{t'})^\theta - 1]$ , which is valid for  $T^+/t' > 1$ . Similar scaling arguments are used for  $\Sigma^+$  in Eq. (9), which lead to  $\Sigma^+ \simeq (T^+)^\theta (t')^{1-\theta}$ , an approximation which is valid for  $t' < T^+$ . For  $t' > T^+$ ,  $N^+ = 0$  and  $\Sigma^+ = T^+$ . In summary and after some rearrangements, we obtain

understand this note that trajectories with short but finite total time in state on ( $T^+ \ll T$ ) will have finite correlation functions when  $t' = 0$ . However, when  $t'$  is increased the corresponding correlation functions will typically decay very fast to zero. On the other hand, correlation functions of trajectories with  $T^+ \sim T$  do not change much when  $t'$  is increased (as long as  $t' \ll T^+$ ). This leads to the gradual nonuniform shift to the left, and “absorption” into  $C_{TA}(t', T') = 0$ , of the Lamperti distribution shape, and hence to a nonsymmetrical shape of the PDFs of the correlation function whenever  $r \neq 0$ .

We now turn to the case  $T \ll t'$ . Since  $t'$  is large we use a decoupling approximation and write Eq. (1) as

$$C_{TA}(t', T') \simeq I_{[0,T]} I_{[t',T']}. \quad (11)$$

We distinguish between two types of trajectories: those in which no transition event occurs in the time interval  $[T, T']$  and all other trajectories. Let  $P_0(a, b)$  be the probability of making no transition between time  $a$  and time  $b$ , also called the persistence probability [3],

$$P_0(a, b) \sim \frac{\sin \pi \theta}{\pi} \int_0^{a/b} x^{\theta-1} (1-x)^{-\theta} dx \quad (12)$$

in the scaling limit. Using the Lamperti distribution for  $I_{[0,T]}$ , and probabilistic arguments with details left to a future publication, we find the PDF of  $C_{TA}(t', T')$ ,

$$P_{C_{TA}(t', T')}(z) \simeq [1 - P_0(T, T')][1 - P_0(t', T')] \\ \times \int_z^1 \frac{l_\theta(x)}{x} dx + \frac{P_0(t', T')}{2} [l_\theta(z) + \delta(z)] \\ + P_0(T, T') \left[ z l_\theta(z) + \frac{\delta(z)}{2} \right]. \quad (13)$$

Note that to derive Eq. (13) we used the fact that  $I_{[0,T]}$  and  $I_{[t',T']}$  are correlated. In Figs. 2 and 3 we plot these PDFs of  $C_{TA}(t', T')$  (solid curves) together with numerical simulations (diamonds) and find good agreement between theory and simulation, for the cases where these approximations are expected to hold,  $r > 1/2$ . In the limit  $t'/T' \rightarrow 1$ , Eq. (13) simplifies to

$$P_{C_{TA}(t', T')}(z) \sim [l_\theta(z) + \delta(z)]/2, \quad (14)$$

a result which is easily understood if one realizes that in this limit  $I_{[t',T']}$  in Eq. (11) is either 0 or 1 with probabilities 1/2, and that the PDF of  $I_{[0,T]}$  is Lamperti's PDF Eq. (8).

Equations (10) and (13) are the main analytical results of the Letter since they give approximate PDFs of the non-ergodic intensity correlation functions for a large range of parameters. We note that the considered nonergodic process cannot be decomposed into ergodic components. Ergodic decomposition means that depending on *a priori* unknown (or randomly selected) initial condition the random process will follow one of many possible nonmixing branches, each of which is assumed ergodic, but with different properties [21,22]. Such a decomposable non-ergodicity may be the case, e.g., for neuronal spike trains [23] and gene expression time series [24], where different neurons or subjects are not necessarily statistically equivalent. In our case, the process is asymptotically insensitive to the initial conditions and clearly mixing. However, the mixing is so slow (its characteristic time diverges) that the time (or sample) average of any realization fluctuates and does not converge.

Finally, we quantified the nonergodicity induced by Lévy walks. The cause of this nonergodicity is the diver-

gence of the mean sojourn time. More generally, time average correlation functions and related power spectra of scale-free time series should be treated with care, and the ergodic hypothesis should not be taken for granted even in seemingly simple processes [25].

This work was supported by National Science Foundation Grant No. CHE-0344930.

- 
- [1] I. Goychuk and P. Hänggi, *Physica (Amsterdam)* **325A**, 9 (2003).
  - [2] G. Zumofen and J. Klafter, *Phys. Rev. E* **47**, 851 (1993).
  - [3] C. Godrèche and J.M. Luck, *J. Stat. Phys.* **104**, 489 (2001).
  - [4] A. Baldassarri, J.P. Bouchaud, I. Dornic, and C. Godrèche, *Phys. Rev. E* **59**, R20 (1999).
  - [5] J. Klafter, M. F. Shlesinger, and G. Zumofen, *Phys. Today* **49**, No. 2, 33 (1996).
  - [6] G. Messin, J.P. Hermier, E. Giacobino, P. Desbiolles, and M. Dahan, *Opt. Lett.* **26**, 1891 (2001).
  - [7] X. Brokmann, J.P. Hermier, G. Messin, P. Desbiolles, J.-P. Bouchaud, and M. Dahan, *Phys. Rev. Lett.* **90**, 120601 (2003).
  - [8] M. Nirmal, B. O. Dabbousi, M. G. Bawendi, J.J. Macklin, J.K. Trautman, T.D. Harris, and L.E. Brus, *Nature (London)* **383**, 802 (1996).
  - [9] M. Kuno, D.P. Fromm, H.F. Hamann, A. Gallagher, and D.J. Nesbitt, *J. Chem. Phys.* **112**, 3117 (2000).
  - [10] K. T. Shimizu, R. G. Neuhauser, C. A. Leatherdale, S. A. Empedocles, W. K. Woo, and M. G. Bawendi, *Phys. Rev. B* **63**, 205316 (2001).
  - [11] J. P. Bouchaud, *J. Phys. I (France)* **2**, 1705 (1992).
  - [12] G. Margolin and E. Barkai, *J. Chem. Phys.* **121**, 1566 (2004).
  - [13] G. Aquino, L. Palatella, and P. Grigolini, *Phys. Rev. Lett.* **93**, 050601 (2004).
  - [14] R. Verberk, A. M. van Oijen, and M. Orrit, *Phys. Rev. B* **66**, 233202 (2002).
  - [15] M. Pelton, D. G. Grier, and P. Guyot-Sionnest, *Appl. Phys. Lett.* **85**, 819 (2004).
  - [16] R. Verberk and M. Orrit, *J. Chem. Phys.* **119**, 2214 (2003).
  - [17] E. Barkai, Y. Jung, and R. Silbey, *Annu. Rev. Phys. Chem.* **55**, 457 (2004).
  - [18] N. Laskin, *Comm. Nonlin. Sci. Num. Sim.* **8**, 201 (2003).
  - [19] Y. Jung, E. Barkai, and R. Silbey, *Chem. Phys.* **284**, 181 (2002).
  - [20] J. Lamperti, *Trans. Am. Math. Soc.* **88**, 380 (1958).
  - [21] R. M. Gray, *Probability, Random Processes, and Ergodic Properties* (Springer-Verlag, New York, 1988).
  - [22] I. V. Basawa and D. J. Scott, *Asymptotic Optimal Inference for Non-ergodic Models* (Springer-Verlag, Berlin, 1983).
  - [23] N. Masuda and K. Aihara, *Neural Comput.* **15**, 1341 (2003).
  - [24] T. G. Dewey, *Drug Discovery Today* **7**, S170 (2002).
  - [25] After this work was completed, a related paper was published: E. Lutz, *Phys. Rev. Lett.* **93**, 190602 (2004).